Journal of Applied Mechanics and Technical Physics, Vol. 35, No. 1, 1994

COMPUTATIONAL ANALYSIS OF A SPATIAL COMPRESSED TURBULENT BOUNDARY LAYER ON THE UPWIND SIDE OF DELTA WINGS UNDER SUPERSONIC FLOW

V. N. Vetlutskii and T. V. Poplavskaya

UDC 532.526

A qualitative study of flow regimes as a function of the sweep χ, the Mach number M_∞, and the angle of attack α under supersonic flow over delta wings with a sharp leading edge was carried out experimentally in [1, 2]. The effect of the angle of attack on the turbulent-laminar transition was studied in [3, 4]. It was shown that the transition for triangular plates with χ = 60-75° accelerates for $\alpha \le 10°$ and is delayed for $\alpha > 15°$. In [5] the Stanton numbers were measured on the upwind side of delta wings for χ = 65, 70°, α = 0-15°, M_∞ = 6.1 and 8. The results of the calculations of laminar and turbulent boundary layers on a flat delta wing are given in [6].

Using the algorithm from [7, 8], below we carry out calculations for the compressed turbulent boundary layer on the upwind side of flat and profiled delta wings for $M_\infty > 1$. The parameters of the laminar-turbulent transition were chosen from a comparison of the distribution of the Stanton numbers with the experimental results [5]. We also study the effect that the determining parameters of the problem have on the distribution of local and overall surface friction coefficients.

1. We consider the turbulent boundary layer on a profiled delta wing, whose leading edge has a sweep χ. Its surface y = G(x, z) is given in Cartesian coordinates x, y, z with origin at the nose of the wing. The plane z = 0 coincides with its symmetry plane. The leading and trailing edges of the wing lie in the plane y = 0; z = f(x) is the equation of the leading edge. The velocity vector of the mainstream lies in the vertical symmetry plane of the wing and makes an angle of attack α with the x axis.

To describe the boundary layer we introduce a nonorthogonal system of coordinates (ξ, η, ζ), bound to the surface of the body:

$$\xi = x, \quad \zeta = 1 - z/f(x).$$

Here the coordinate ζ is reckoned from the leading edge in the section ξ = const; η is the normal to the surface. The components u, v, w correspond to the coordinates ξ, η, ζ. The complete equations of the compressed boundary layer in the variables ξ, λ, ζ, where $\lambda = \eta/\sqrt{\xi}$ and the boundary conditions for the region Ω ($\xi \ge \xi_0$, $0 \le \zeta \le \zeta_k$, $0 \le \lambda \le \lambda_e(\xi, \zeta)$) are written out in [7, 8].

The section $\xi = \xi_0$ is given at the conical nose of the body and the profiles u_0, w_0, T_0 are taken from the self-similar solution for the nose. At the leading edge ($\zeta = 0$) the profiles u_δ, w_δ, T_δ are determined from the solution of the ordinary differential equations obtained from the complete equations of the boundary layer by the passage to the limit $\zeta \to 0$ on the assumption that all the sought functions and their derivatives are bounded. The usual attachment conditions for a viscous fluid and given at the surface of the body ($\lambda = 0$) and the gas and the wall are assumed to be at the same temperature $T = T_w$. At the outer boundary ($\lambda = \lambda_e(\xi, \zeta)$) the parameters of the boundary layer are taken from calculations of the flow of nonviscous gas over the wing. The results given below were calculated for χ = 70° by taking the data obtained by the method of [9] and those for χ = 45° by taking data from [10].

The turbulent viscosity coefficient μ_t was added to the molecular viscosity coefficient μ in the turbulent flow calculation. The heat-conduction coefficient k was changed in similar fashion. The overall viscosity and heat-conduction coefficients are thus calculated from

Novosibirsk. Translated from Prikladnaya Mekhanika i Tekhnicheskaya Fizika, No. 1, pp. 68-74, January-February, 1994. Original article submitted February 18, 1993.

0021-8944/94/3501-0069$12.50

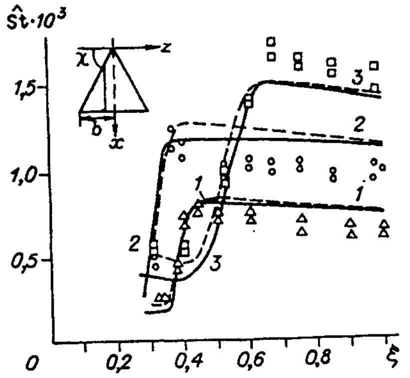

Fig. 1

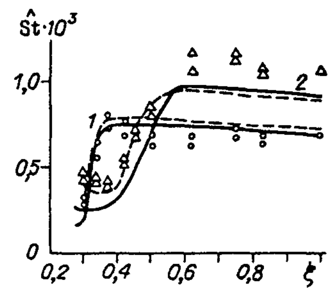

Fig. 2

TABLE 1

χ	α	Re_L	cf_x	r_1	r_2
deg					
65	5	$1{,}38\cdot10^7$	0,00195	200	400
	10	$1{,}38\cdot10^7$	0,00337	120	320
		$4{,}73\cdot10^6$	0,00294	150	450
70	5	$1{,}59\cdot10^7$	0,00205	150	350
		$5{,}5\cdot10^6$	0,00198	130	400

$$\mu_\Sigma = \mu + \Gamma\mu_t, \quad k_\Sigma = \frac{c_p}{\mathrm{Pr}}\left(\mu + \Gamma\frac{\mathrm{Pr}}{\mathrm{Pr}_t}\mu_t\right),$$

where Pr and Pr_t are the molecular and turbulent Prandtl numbers; Γ is the laminar-turbulent transition coefficient, which is determined by the dependence of the Reynolds number on the mainstream parameters and the momentum thickness $\mathrm{Re}_{\delta^{**}}$ on the local Mach number M_e [11]:

$$\Gamma = \begin{cases} 0, & \text{if} \quad r < r_1, \\ 1 - \exp\left(-6{,}5\left((r - r_1)/(r_2 - r_1)\right)^2\right), & \text{if} \quad r > r_1. \end{cases}$$

Here $r = \mathrm{Re}_{\delta^{**}}/\exp(0.2\ M_e)$; the values of r_1 and r_2 correspond to the onset and end of the transition.

For the calculation of turbulent flow the value of μ_t was set on the basis of the hypothesis of the displacement path length in the form

$$\mu_t = \rho l^2\sqrt{\left(\frac{\partial u}{\partial\zeta}\right)^2 + \left(\frac{\partial w}{\partial\zeta}\right)^2 + 2\frac{\partial u}{\partial\zeta}\frac{\partial w}{\partial\zeta}\cos\varphi},$$

where l is the displacement path length; φ is the angle between the ξ and ζ axes; and ρ is the density. In our study we use an algebraic model of turbulent viscosity, i.e., the model of Michel [12] with the following expression for the displacement path length:

$$l/\delta = 0{,}09\ \mathrm{th}\ [0{,}435/0{,}09\ (y/\delta)]F, \quad F = 1 - \exp\left(-\frac{y\sqrt{\tau_w\rho_w}}{26\,\mu_w}\right).$$

TABLE 2

Variant	r_1	r_2	CF_x
1	150	450	0,00294
2	150	350	0,00315
3	230	500	0,00207

TABLE 3

M_∞	χ, deg	α, deg	Flow regime	Profile thickness c	CF_x	CF
6	45	0	*AI*	0	0,00117	0,00117
				0,03	0,00123	0,00283
		5	*AI*	0	0,00195	0,00885
				0,03	0,00199	0,0127
		10	*AI*	0	0,00303	0,0282
				0,03	0,00314	0,0331
	70	0	*AI*	0	0,00125	0,00125
		5	*AI*	0	0,00212	—
		10	*BI*	0	0,00316	—
		15	*BI*	0	0,00427	—
4	70	5	*BI*	0	0,00268	—
8	70	5	*AI*	0	0,00170	—

Here F is the Van Drist damping factor in the boundary region; δ is the thickness of the boundary layer; τ_w is the length of the viscous stress vector on the wall. Elsewhere [13] we showed that the turbulence models of Michel [12], Cebeci and Smith [14], and Pletcher [15] give similar values of the viscous stress for the boundary layer on an oval-cylindrical body.

The system of boundary layer equations was solved numerically by means of the implicit difference scheme described in [16]. The following computational algorithm was used to solve the difference equations. First, the self-similar boundary large on the conical part was calculated by the march method over the ζ coordinate [7]. The resulting values of the gasdynamic parameters u_0, w_0, T_0 were assigned as the initial conditions in the section $\xi = \xi_0$ on the conical section. Then, using the march method over the ξ method, we solved the three-dimensional boundary-layer equation on the rest of the wing surface.

The velocity and temperature components calculated in the boundary layer of the sections were used to calculate the components of the friction stress coefficients c_{f_1} and c_{f_2} and the Stanton number on the wing surface. The formulas for them are given in [8, 17]. Since these parameters become infinite at the leading edge, we henceforth give $\hat{c}_f = c_f\sqrt{\zeta}$ and $\hat{S}t = St\sqrt{\zeta}$. We also determined the contribution of the friction forces CF_x and CF_y to the coefficients of the longitudinal and normal aerodynamic forces acting on the wing. The formulas for them are given [8, 17].

2. The algorithm and the computational program were verified by comparing the calculated values of $\hat{S}t$ on the upwind side of flat wings with the experimental values [5]. Table 1 shows the variants for which this comparison was made in the section $z = 0.25b$, parallel to the symmetry plane of the flow, where b is half the wingspan. Here for both wings $M_\infty = 6.1$ and the wall/mainstream temperature ratio $T_w/T_\infty = 4.39$, which corresponds to a relative enthalpy $H_w/H_\infty = 0.535$. The last columns give the values of the parameters of the beginning and the end of the transition r_1 and r_2, chosen from the condition of best agreement of the Stanton numbers with the experimental values. The distributions of $\hat{S}t$ in this section for wings with sweep $\chi = 65°$ are given in Fig. 1 and with $\chi = 70°$, in Fig. 2. Curves 1 and 2 in Fig. 1 represent calculations for $\alpha = 5$, $10°$ and Reynolds number $Re_L = 1.38 \cdot 10^7$ (here Re_L was calculated from the mainstream parameters and the length of the center chord L); corresponding to them are the triangles and circles, indicating data from [5]. Curve 3 and the small squares pertain to the variant for $\alpha = 10°$ and $Re_L = 4.73 \cdot 10^6$. Figure 2 shows the results for $\alpha = 5°$ and $Re_L = 1.59 \cdot 10^7$ (curve 1 and circles) and $Re_L = 5.5 \cdot 10^6$ (curve 2 and triangles). As seen from Figs. 1 and 2, the calculated and experimental data differ by less

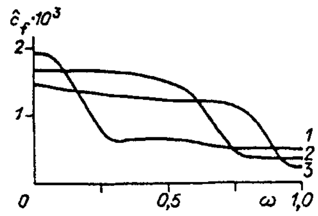

Fig. 3

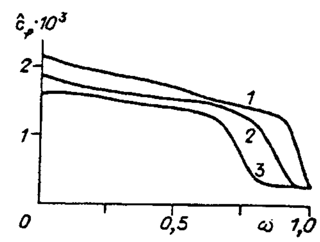

Fig. 4

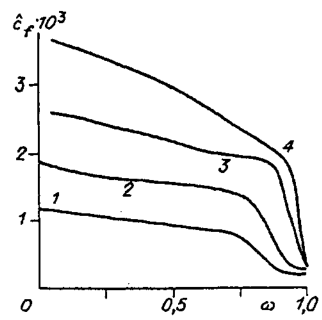

Fig. 5

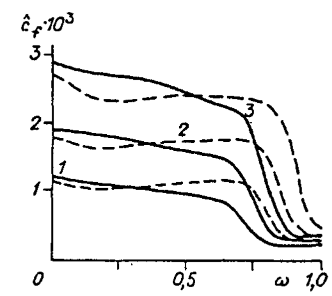

Fig. 6

than 15% in the turbulent-flow region. The dashed lines in Figs. 1 and 2 represent the results of calculations in [5] by the theory of plane sections. As mentioned in [5], the difference between the calculated and experimental Stanton numbers reaches 20%.

The correct choice of r_1 and r_2 is important for best agreement with experiments. It is not clear beforehand, however, what that choice should be in one case or another. Accordingly, three variants of calculations were carried out with different values of these parameters (Table 2) for a wing when $\chi = 65°$, $M_\infty = 6$, $\alpha = 10°$, $Re_L = 4.73 \cdot 10^6$, $T_w/T_\infty = 4.39$. In the first variant we chose r_1 and r_2 from the condition of best agreement of the distribution of $\hat{S}t$ with experimental data, in the second we took their average values for a series of calculations (see Table 1), and in the third we took values slightly out of their range in Table 1. As is seen from Table 2, the value of the overall coefficient CF_x in the second variant differs from the first by 6%, while in the third it differs by more than 30%. In calculations of the boundary layer on the upwind side of a delta wing for parameters close to those in Table 1, therefore, the average can evidently be taken for the transition parameters: $r_1 = 150$ and $r_2 = 350$. Just such values were used in subsequent variants.

3. We have done a number of calculations here to ascertain the effect of the determining parameters on a turbulent boundary layer. The values of the latter for the main variants calculated are given in Table 3 for $Re_L = 1.5 \cdot 10^7$ and $H_w/H_\infty = 0.535$. For profiled wings the equation of the surface has the form

$$G(\xi, \zeta) = 4c\,(1 - (1 - \zeta)^2)\,(1 - \xi)\,\xi^{1.047},$$

where c is the relative thickness of the profile [10]. All the calculations were done with a single program, which worked successfully for regime A1, when the shock wave is attached to the leading edges, and for regime B1 with detached shock wave, when the dividing streamline comes at the leading edge [18].

Figures 3-6 show the distributions of the local friction coefficient $\hat{c}_f$ as a function of the parameter $\omega = 1 - \zeta$, which corresponds to the relative distance from the symmetry plane in the wing cross section. The development of the boundary layer by sections is clearly visible in Fig. 3, where the distribution of $\hat{c}_f$ is given for $\xi = 0.2$, 0.4, and 1.0 (curves 1-3) for $\chi = 70°$, $M_\infty = 8$, $\alpha = 5°$, and $c = 0$. The transition to turbulent flow begins here near the symmetry plane and, moving to the trailing edge, extends to practically the entire wing surface. The flow remains laminar in the vicinity of the leading edges, as it should.

With increasing Mach number the transition to turbulent flow is delayed and the region of turbulent flow decreases. This is seen clearly from Fig. 4, which shows the distribution of $\hat{c}_f$ on the wing surface in the section $\xi = 0.5$ for $\chi = 70°$, $\alpha =$

5°, c = 0, and M_∞ = 4, 6, 8 (curves 1-3). The region of laminar is very small here for M_∞ = 4. We also see that the absolute values of $\bar{c}_f$ decrease as the Mach number increases. All of this supports our earlier results for $Re_L = 2 \cdot 10^6$ [8].

The effect of the angle of attack on the boundary-layer parameters is illustrated in Fig. 5 for a flat wing with $\chi = 70°$ and in Fig. 6 for flat (solid lines) and profiled (dashed lines) wings with $\chi = 45°$. Curves 1-3 in both figures correspond to ξ = 0.5 and α = 0, 5, 10° and curve 4 (Fig. 5) corresponds to $\alpha = 15°$. The graphs indicate that $\bar{c}_f$ is a monotonic function of the angle of attack. The region of turbulent flow increases with the angle of attack and the zone of the transition shifts to the nose of the wing. Regime B1 is realized for $\chi = 70°$ and α = 10, 15° (curves 3, 4 in Fig. 5) and the region of laminar flow near the edges is very small.

For a flat wing with $\chi = 45°$ (Fig. 6, solid curves) the values of $\bar{c}_f$ near the symmetry plane virtually coincide with their values for the wing with $\chi = 70°$. The region of laminar flow at the leading edges, however, is larger in this case.

Comparing the $\bar{c}_f$ distributions for flat and profiled (dashed lines) wings for different angles of attack, we come to the conclusion that the region of turbulent flow is larger in the second case. The absolute value of $\bar{c}_f$ in this region, however, is slightly lower, as is particularly noticeable for $\alpha = 10°$ (curves 3).

In conclusion we analyze the contribution of the total friction forces CF_x on the upwind side to the coefficient of the longitudinal aerodynamic force CF. Their values are given in the last two columns of Table 3. When the sweep of the flat wing is increased from 45° to 70° the coefficient CF_x increases slightly (3-7%) for all angles of attack, which is consistent with the analogous dependence for a completely laminar boundary layer on the wing [18]. The value of CF_x decreases by 37% when the Mach number grows from 4 to 8 for $\chi = 70°$ and $\alpha = 5°$.

As in the case of a completely laminar boundary layer [17], CF_x is slightly higher on a profiled wing than on a flat wing. Although the difference does decrease from 5 to 1% as the angle of attack increases, the wave resistance grows substantially and as a result the contribution of CF_x to the total resistance of the wing with $\chi = 45°$ decreases from 100 to 43% for $\alpha = 0$, from 23 to 17% for $\alpha = 5°$, and from 11 to 9% for $\alpha = 15°$.

In summary, in this study we have analyzed the effect of the determining parameters of the problem on the local and overall friction coefficients on the surface of a delta wing.

REFERENCES

1. V. Ya. Borovoi, B. A. Ivanov, A. A. Orlov, and V. N. Karchenko, "Study of the flow of a supersonic stream over wings of different shape in the plane by the laser knife method," Tr. TsAGI, No. 1793 (1977).
2. L. C. Squire, "Flow regimes over delta wings at supersonic and hypersonic speeds," Aeronaut. Quart., **27**, No. 1 (1976).
3. N. A. Davydova and A. Ya. Yushin, "Experimental study of the effect of the angle of attack on the laminar-turbulent transition of a boundary layer near the lower surface of a triangular plate with open edges," Uch. Zap. TaAGI, **6**, No. 1 (1975).
4. N. A. Kovaleva, N. P. Kolina, and A. Ya. Yushin, "Effect of the angle of attack on the laminar-turbulent transition of a boundary layer on the lower surface of a triangular plate in a supersonic stream of gas," Uch. Zap. TaAGI, **21**, No. 4 (1990).
5. N. A. Kovaleva, N. P. Kolina, A. P. Kosykh, and A. Ya. Yushin, "Results of experimental and numerical studies of aerodynamic heating of the lower surface of sharp leading-edge delta wings for M_∞ = 6.1 and 8," Izv. Akad. Nauk SSSR Mekh. Zhidk. Gaza, No. 4 (1991).
6. G. A. Shcheckin, "Numerical calculation of a three-dimensional boundary layer in the laminar and turbulent regions on wings at supersonic flight speeds," in: Experimental and Theoretical Studies of the Aerodynamics of Elements of Aircraft and Its Parts [in Russian], Moscow Aviation Institute, Moscow (1983).
7. V. N. Vetlutskii and T. V. Poplavskaya, "On the calculation of a laminar compressed boundary layer on a profiled delta wing with supersonic leading edges," Model Mekh., **3**(20), No. 6 (1989).
8. V. N. Vetlutskii and T. V. Poplavskaya, "Calculation of a three-dimensional turbulent boundary layer on profiled delta wings," Model. Mekh., **6**(23), No. 1 (1992).
9. A. P. Shashkin and V. F. Volkov, "One scheme for numerical calculation of nonviscous gasdynamic flows," in: Problems of Flow over Bodies with Three-Dimensional Configurations [in Russian], Institute of Theoretical and Applied Mechanics, Novosibirsk (1978).

10. G. P. Voskresenskii, A. S. Il'ina, and V. S. Tatarenchik, "Supersonic flow over wings with attached shock wave," Tr. TsAGI, No. 1590 (1974).
11. N. Thyson, J. Neuringer, A. Pallone, and K. K. Chen, "Nose tip shape change predictions during atmospheric reentry," Pap./AIAA No. 70-827, New York (1970).
12. R. Michel, J. Cousteix, and C. Quemard, "Application d'un schéma améliore de longuer de mélange à l'étude de couches limites turbulentes tridimensionnelles," AGARD Meeting on Turbulent Shear Flows, London (1971).
13. V. N. Vetlutsky and E. Krause, "Berechnung dreidimensionaler Grenzschichten an spitzern Korpern," Abhandl. Aerodyn. Inst. der RWRH Aachen, Aachen (1990).
14. T. Cebeci and A. M. O. Smith, Analysis of Turbulent Layers, Academic Press, New York (1974).
15. R. H. Pletcher, "On a finite difference solution for the constant property turbulent boundary layer," AIAA J., No. 7 (1969).
16. V. N. Vetlutsky, "Laminar boundary layer on a flat plane with rotating cylinder," Computers and Fluids, No. 9 (1981).
17. V. N. Vetlutskii and T. V. Poplavskaya, "Numerical calculation of a three-dimensional compressed boundary layer on profiled delta wings with supersonic leading edges," Prikl. Mekh. Tekh. Fiz., No. 5 (1993).
18. V. N. Vetlutskii and T. V. Poplavskaya, "A compressed laminar boundary layer on a triangular plate with attached shock wave," Prikl. Mekh. Tekh. Fiz., No. 5 (1985).